Societal vulnerability amplifies the severity of global groundwater risk and creates latent hotspots

Sara Nazari[1,2,3,4 *], Robert Reinecke[5], Inge E. M. de Graaf[4], Dor Fridman[3], Bárbara A. Willaarts[3], Nils Moosdorf[1,2]

[1]Leibniz Centre for Tropical Marine Research (ZMT), Bremen, Germany
[2]Institute of Geosciences, Kiel University, Kiel, Germany
[3]Water Security Research Group, Biodiversity and Natural Resources Program, International Institute for Applied Systems Analysis (IIASA), Laxenburg, Austria
[4]Earth Systems and Global Change Group. Wageningen University and Research, Wageningen, The Netherlands
[5]Institute of Geography, Johannes Gutenberg-University Mainz, Mainz, Germany
[*] Correspondence to sara.nazari@leibniz-zmt.de

Supplementary Text

1. Societal vulnerability assessment of the global groundwater risk framework

In the groundwater risk framework, vulnerability reflects the societal conditions that shape the ability to cope with and adapt to groundwater stress (hazard). More generally, the Hyogo Framework for Action defines vulnerability as "the conditions determined by physical, social, economic and environmental factors or processes which increase the susceptibility of a community to the impact of hazards"[1]. In our context, vulnerability captures the socio-economic resilience, water and resources dependency, and water governance frameworks that influence how severely groundwater stress may translate into risk.

The selection of indicators was guided by a combination of expert consultation and a review of established risk assessment frameworks[2-6]. Expert input was provided by the author team, drawing on interdisciplinary expertise in groundwater hydrology, water resources management, and socio-environmental risk assessment. In an initial screening, 28 indicators were selected as potentially relevant to represent societal vulnerability to groundwater stress. These covered a broad set of socio-economic and governance dimensions. Each indicator was then evaluated against several criteria, including: (i) global data availability, (ii) completeness and consistency of coverage across regions, (iii) temporal representativeness for the study period (2001–2020), and (iv) spatial resolution suitable for integration with other components of the framework. Particular emphasis was placed on selecting datasets that are publicly accessible at the global scale, thereby ensuring transparency, reproducibility, and the potential for future updates as new data become available. Based on this evaluation, the set was narrowed to 14 indicators (Supplementary Table 1).

Assigning weights to vulnerability indicators is a critical step, but also one of the most challenging. There is no universally accepted weighting method[7], and equal-weighting approaches, while simple and transparent, risk ignoring the fact that different indicators may contribute unequally to societal vulnerability[8,9]. To address this, we employed Principal Component Analysis (PCA), a statistical technique that objectively derives indicator weights by analysing the variance structure of the data and reducing partly correlated variables into smaller sets of uncorrelated components [9,10]. PCA has been widely applied in vulnerability index assessments[8,11-13] because it allows for data-driven weighting and the identification of underlying vulnerability dimensions.

The vulnerability indicators (Supplementary Table 1) were first harmonized to the analysis grid (0.1°) through up- or downscaling where necessary. Missing values were gap-filled using indicator-specific approaches described in Supplementary Table 1. All indicators were then standardized using z-score normalization, ensuring comparability across variables with different units. PCA was performed and followed by varimax rotation with Kaiser normalization[8,14]. To evaluate the adequacy and robustness of the dataset for PCA, we applied two diagnostic tests : (i) the Kaiser–Meyer–Olkin (KMO)[15] measure of sampling adequacy, with values above 0.80 considered suitable, and (ii) Bartlett's test of sphericity[16], which tests the null hypothesis ($p < 0.05$) of no correlation among indicators[15,17,18]. Only when these tests confirmed adequacy was PCA retained for constructing the vulnerability index.

From the rotated component matrix, indicators with factor loadings ≥ 0.5 were retained for each component. Weights for each indicator were derived from their factor loadings, while the contribution of each vulnerability dimension was weighted by the share of variance it explained relative to the total variance. The resulting composite index therefore reflects both the contribution of individual indicators and the relative importance of the broader vulnerability dimensions.

Applying PCA to the vulnerability indicators revealed several statistically independent components. These components were subsequently interpreted and grouped into higher-level vulnerability dimensions based on their conceptual coherence: socio-economic resilience, water governance frameworks, and water and resources dependency. The first principal component is dominated by socio-economic indicators, including GDP[19], HDI[20], food insecurity[21], poverty[22], and access to unimproved water[4,23]. Governance-related indicators primarily load onto the second component. Several additional components, each explaining a smaller share of variance, capture complementary aspects of dependence on water resources, infrastructure, energy access, and withdrawals costs; these components were therefore grouped to define a single water and resources dependency dimension. Together, the retained components account for approximately 90% of the total variance (Supplementary Table 2).

2. Infrastructure Availability for Alternative Water Sources (IAAWS)

To represent societal coping capacity in the event of reduced groundwater availability, we developed a global dataset of Infrastructure Availability for Alternative Water Sources (IAAWS). This dataset integrates three major sources of alternative water supply: dam storage[24], desalinated water production[25,26], and wastewater reuse[27] and translates them into a per-capita indicator at 0.1° spatial resolution. The data development process consisted of the following steps:

- Input datasets:

    I. Dam capacity was obtained from the Global Dam Watch database[24], which provides dam locations and storage capacities as point shapefiles.

    II. Desalinated water production was derived from Hanasaki, et al. [25] and Ai, et al. [26], available at 0.5° resolution, representing seawater desalination weighted by population density along coastlines.

    III. Wastewater reuse was taken from a data-driven model (at 0.08° resolution) estimating domestic and manufacturing wastewater reuse [27].

- Aggregation to river basins: Using river basins[4], the summed capacity of all dams within each basin was added to the values of desalinated water production and wastewater reuse (expressed in m^3).

- Per-capita availability: The combined alternative water supply per basin was divided by the basin population from GPWv4 (year 2015)[28], which matches the reference year of the desalination and wastewater datasets. This produced a per-capita estimate of alternative water availability for each basin.

- Downscaling to grid level: Basin-level per-capita values were uniformly downscaled to 0.1° grid cells to align with the spatial resolution of the groundwater risk framework.

- Ranking: Grid-level values were converted into global decile ranks, allowing comparison across regions. This highlight relative differences in infrastructure availability worldwide rather than absolute magnitudes (Supplementary Fig. 8).

- Use in vulnerability assessment: In the vulnerability framework, IAAWS was treated as a coping capacity indicator and inverted so that low infrastructure availability corresponds to higher vulnerability. Regions with substantial populations but zero alternative supply per capita were assigned the lowest rank.

3. Sensitivity analysis of groundwater risk to recharge and withdrawal changes

To evaluate the sensitivity of groundwater risk to changes in hazard, we conducted a perturbation-based sensitivity analysis focusing on two key drivers: declining groundwater recharge and increasing groundwater withdrawals. The objective was to assess how plausible changes in recharge associated with climate change, and increases in withdrawals linked to human pressures on aquifers, propagate through the risk framework when integrated with exposure and societal vulnerability.

- General approach and baseline definition: The sensitivity analysis isolates the effect of hazard changes by holding exposure and vulnerability constant at their grid-level baseline values. Owing to the absence of projections for future relative rate of change in withdrawals compared to recharge, the trend component of the hazard formulation was excluded from this analysis. Hazard was therefore represented solely by the long-term average withdrawal-to-recharge ratio. A baseline (current) hazard was first calculated and normalized using the 5th and 95th percentiles. This was then multiplied by the baseline exposure and vulnerability values to estimate the risk.

- Recharge sensitivity experiment: To assess sensitivity to declining recharge, groundwater recharge was systematically reduced while groundwater withdrawals were held constant. Based on the literature reporting regionally variable but potentially substantial reductions in recharge under climate change[29,30], recharge was decreased in incremental steps of 1 mm, up to a maximum reduction of 50 mm. For each recharge-reduction step, a new long-term average withdrawal-to-recharge ratio was calculated and subsequently normalized using the same percentile-based approach as for the baseline. Groundwater risk corresponding to each recharge scenario was then estimated by multiplying this hazard by the fixed exposure and vulnerability datasets.

- Withdrawal sensitivity experiment: To assess sensitivity to increasing groundwater withdrawals, withdrawals were incrementally increased while recharge was held constant. As global projections of future groundwater withdrawals are not available, the parameter range was informed by observed historical changes. Based on evaluating the global groundwater withdrawal increase over the period 2001–2020[31,32], withdrawals were increased in steps ranging from 0.01 to 1 mm. For each withdrawal-increase step, hazard was recalculated,

normalized, and integrated with exposure and vulnerability to derive the corresponding risk estimates, following the same procedure as in the recharge sensitivity experiment.

- Regional hotspot sensitivity assessment: To quantify regional-scale sensitivity, changes in the spatial extent of groundwater risk hotspots for each IPCC region[33] were evaluated. For the baseline and for each recharge- and withdrawal-perturbation scenario, the number of grid cells classified as risk hotspots was calculated within each region. Groundwater risk hotspots were defined using a percentile-based threshold derived from baseline conditions. Specifically, grid cells with baseline risk values exceeding the 75th percentile of the global risk distribution were classified as hotspots. This threshold was held constant across all sensitivity scenarios, such that a grid cell was identified as a hotspot in a given recharge- or withdrawal-perturbation experiment if its simulated risk exceeded the baseline 75th-percentile threshold. Finally, Sensitivity was expressed as change in number of hotspot grid cells in percent, relative to baseline conditions, providing a consistent metric for comparing risk hotspot expansion speed under increasing hazard pressure.

Supplementary Tables

Supplementary Table. 1. Indicators used to construct the vulnerability component.

Indicator	Unit	Spatial Res.	Temporal Res.	Gap-Filling	Source
Gross Domestic Product (GDP) Per Capita	USD	0.08°	1990-2022 (1)	Not applied	Kummu, et al. [19]
Human Development Index (HDI)	Index (0-1)	0.08°	1990-2015 (1)	Not applied	Kummu, et al. [20]
Prevalence of moderate or severe food insecurity	%	National	2020	Class average (2)	SDG 2.1.2 [21]
Poverty headcount ratio at 2.15 $	%	Subnational	2010	National or Class average	World Bank. [22]
Access to unimproved water	%	Hybrid (3)	2015	Not applied	Kuzma, et al. [4];Deshpande, et al. [23]
Groundwater dependency (groundwater withdrawal/total freshwater withdrawal)	%	National	2001-2020 (1)	Model substitution (4)	FAO. [34];Nazari, et al. [35]
External freshwater dependency (total renewable water resources originating outside the country)	%	National	2001-2020 (1)	Not applied	FAO. [34]
Infrastructure availability for alternative water sources (5)	Categorical index	Hybrid	2015	Not applied	Lehner, et al. [24];Hanasaki, et al. [25];Ai, et al. [26];Jones, et al. [27]
Pumping cost	USD/Well per year	0.5°	Spatial extrapolation	Not applied	Niazi, et al. [36]
Access to electricity (6)	kWh per capita, Categorical index	0.008°	1992-2019 (1)	Not applied	CIESIN [28];Hu, et al. [37]
National water resources policy	%	National	2020 (7)	Class average (2)	SDG 6.5.1[38]
Basin/aquifer management plans or similar, based on IWRM (8)	%	National	2020 (7)	Class average (2)	SDG 6.5.1[38]
Basin/aquifer organizations for leading implementation of IWRM	%	National	2020 (7)	Class average (2)	SDG 6.5.1[38]
Proportion of cooperation in TBAs operational arrangement (8)	%	National	2020 (7)	Not applied	SDG 6.5.2[39],IGRAC [40]

(1) Data are provided annually; in this study, values from 2001 to 2020 were averaged.
(2) Countries were classified by income group, region, and aridity. For countries with missing data, the class average was calculated and assigned to the corresponding national level.
(3) This dataset was compiled from Deshpande, et al. [23], which provides 0.04° data for low-income countries, and Kuzma, et al. [4], which provides basin-level data. Where the first dataset was unavailable, the second was used.
(4) When national groundwater withdrawal data were not available from FAO, estimates were derived using modeled national totals based on Nazari, et al. [32]
(5) This dataset was developed in this study to represent the availability of alternative water resource infrastructure. Details are provided in the Supplementary Information (Section 2. Fig. 8).
(6) This dataset was estimated using global electricity consumption data from Hu, et al. [37], combined with population data from CIESIN [28] to derive per-capita values. Grid-level values were subsequently converted into global decile ranks to facilitate comparison across regions and to emphasize relative differences in access to electricity rather than absolute magnitudes.
(7) Data availability varied across years (2017–2023). If values for 2020 were missing, those from 2023 were assigned; if 2023 was also unavailable, 2017 values were used.
(8) IWRM: Integrated Water Resource Management, TBAs: Transboundary Aquifer

Supplementary Table. 2. Principal component analysis (PCA) results.

These results are used to derive vulnerability dimensions, showing the indicator loadings and dimension weights applied when estimating the societal vulnerability index within the groundwater risk framework.

Dimension	Indicator	PC	Weight			PC	% of Variance	Cumulative %
			Indicator	Component	Dimension			
Socio-economic resilience	GDP (1)	PC1	0.89	-	0.46	PC1	41.62	41.62
	HDI (2)	PC1	0.73	-		PC2	12.22	53.84
	Prevalence of food insecurity	PC1	0.63	-		PC3	9.94	63.78
	Poverty headcount ratio at 2.15$	PC1	0.93	-		PC4	7.64	71.42
	Access to Unimproved Water	PC1	0.62	-		PC5	6.86	78.28
						PC6	5.20	83.48
Water governance frameworks	National water resources policy	PC2	0.94	0.72	0.19	PC7	4.75	88.23
	Aquifer management plans	PC2	0.82			PC8	2.72	90.95
	Aquifer level IWRM (3) implementation	PC2	0.81			PC9	2.41	93.36
	TBAs (4) management	PC7	0.98	0.28		PC10	1.71	95.07
						PC11	1.53	96.60
Water and resources dependency	External freshwater dependency	PC3	0.93	0.31	0.35	PC12	1.45	98.05
	Groundwater dependency	PC4	0.97	0.24		PC13	1.19	99.24
	Water infrastructure availability	PC5	0.93	0.21		PC14	0.76	100
	Access to electricity	PC6	0.91	0.16		Kaiser–Meyer–Olkin (KMO)		0.877
	Pumping Cost	PC8	1.00	0.08		Bartlett's test of sphericity		*P < 0.00*

(1) Gross Domestic Product (GDP) Per Capita
(2) Human Development Index (HDI)
(3) IWRM: Integrated Water Resource Management
(4) TBAs: Transboundary Aquifer

Supplementary Table. 3. Names and acronyms of the IPCC reference regions.

Region*	Acronym	Region*	Acronym
N.W.North-America	NWN	N.Central-America	NCA
C.Australia	CAU	N.W.South-America	NWS
N.E.North-America	NEN	E.Europe	EEU
N.Australia	NAU	New-Zealand	NZ
Russian-Far-East	RFE	N.Eastern-Africa	NEAF
S.South-America	SSA	S.Eastern-Africa	SEAF
Madagascar	MDG	E.Southern-Africa	ESAF
W.Southern-Africa	WSAF	S.E.Asia	SEA
N.South-America	NSA	Caribbean	CAR
E.Siberia	ESB	S.Central-America	SCA
Tibetan-Plateau	TIB	S.E.South-America	SES
S.Australia	SAU	N.E.South-America	NES
N.Europe	NEU	E.North-America	ENA
South-American-Monsoon	SAM	Mediterranean	MED
W.Siberia	WSB	W.C.Asia	WCA
E.Australia	EAU	Western-Africa	WAF
E.C.Asia	ECA	E.Asia	EAS
S.W.South-America	SWS	Arabian-Peninsula	ARP
Central-Africa	CAF	West&Central-Europe	WCE
W.North-America	WNA	S.Asia	SAS
Sahara	SAH	C.North-America	CNA

* IPCC WGI reference regions (version 4)[33].

Supplementary Figures

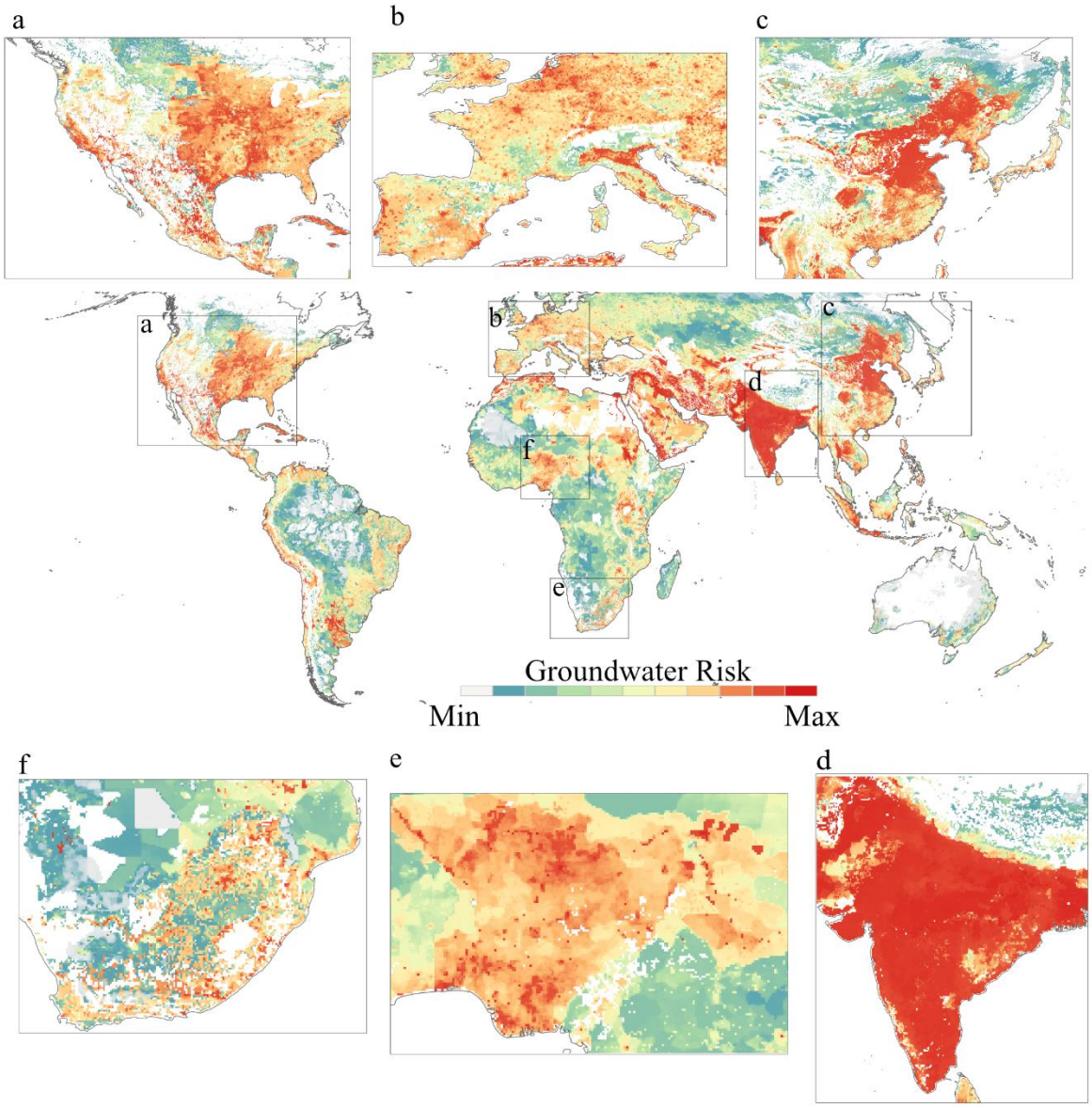

Supplementary Fig. 1. Global distribution of grid-scale groundwater risk.

Groundwater risk is shown at 0.1° spatial resolution and defined as the multiplicative product of hazard, exposure, and societal vulnerability. Colors indicate relative risk levels expressed as percentiles of the global risk distribution, ranging from low to high.

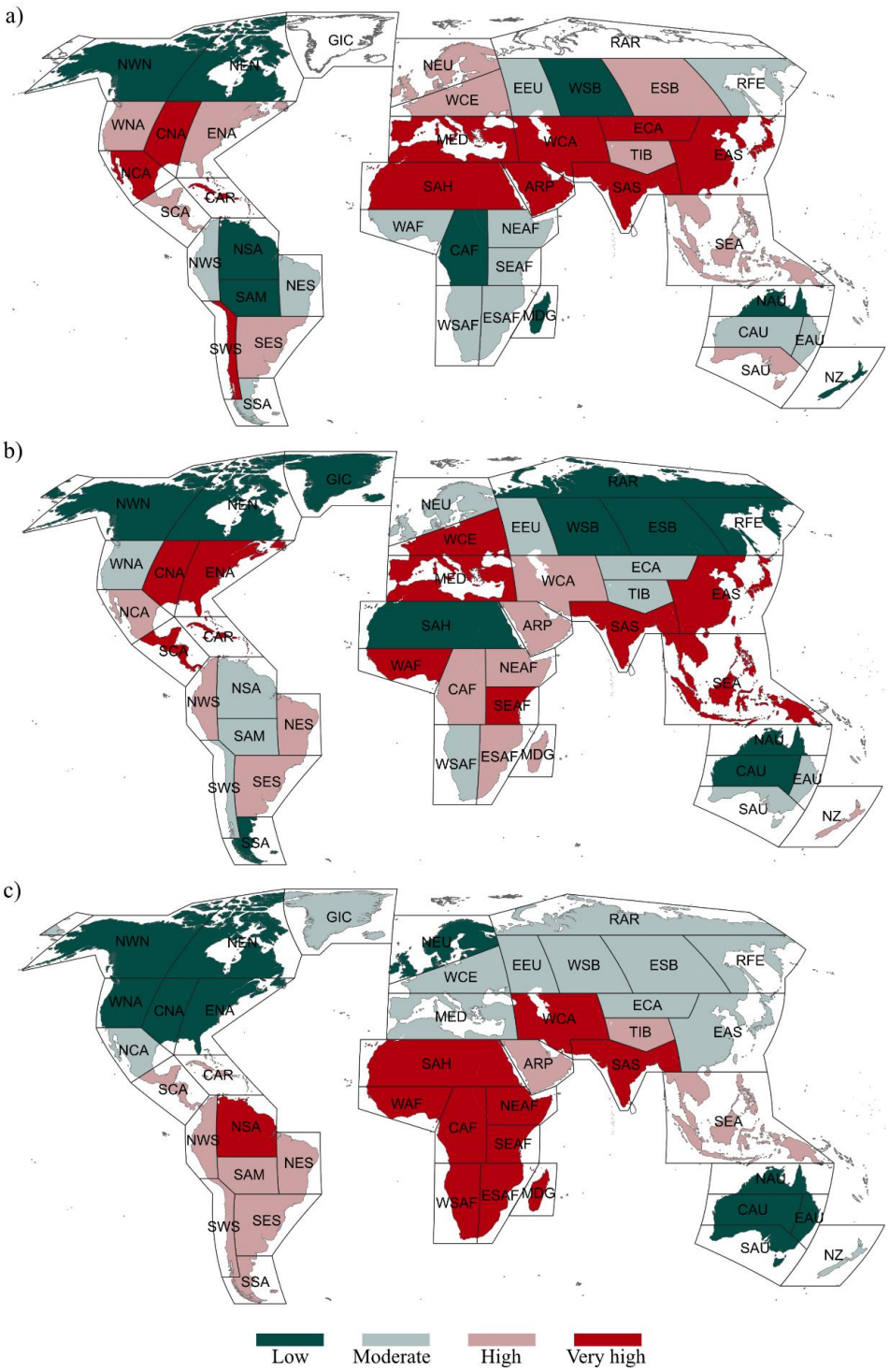

Supplementary Fig. 2. Regional classification of groundwater risk components.

Grid-scale values of the groundwater risk components aggregated to IPCC WGI reference regions (version 4)[33]. Panels show regional classifications of (a) hazard, (b) exposure, and (c) societal vulnerability. For each component, regional values are classified into quartiles of their global distributions and grouped into four categories: low, moderate, high, and very high.

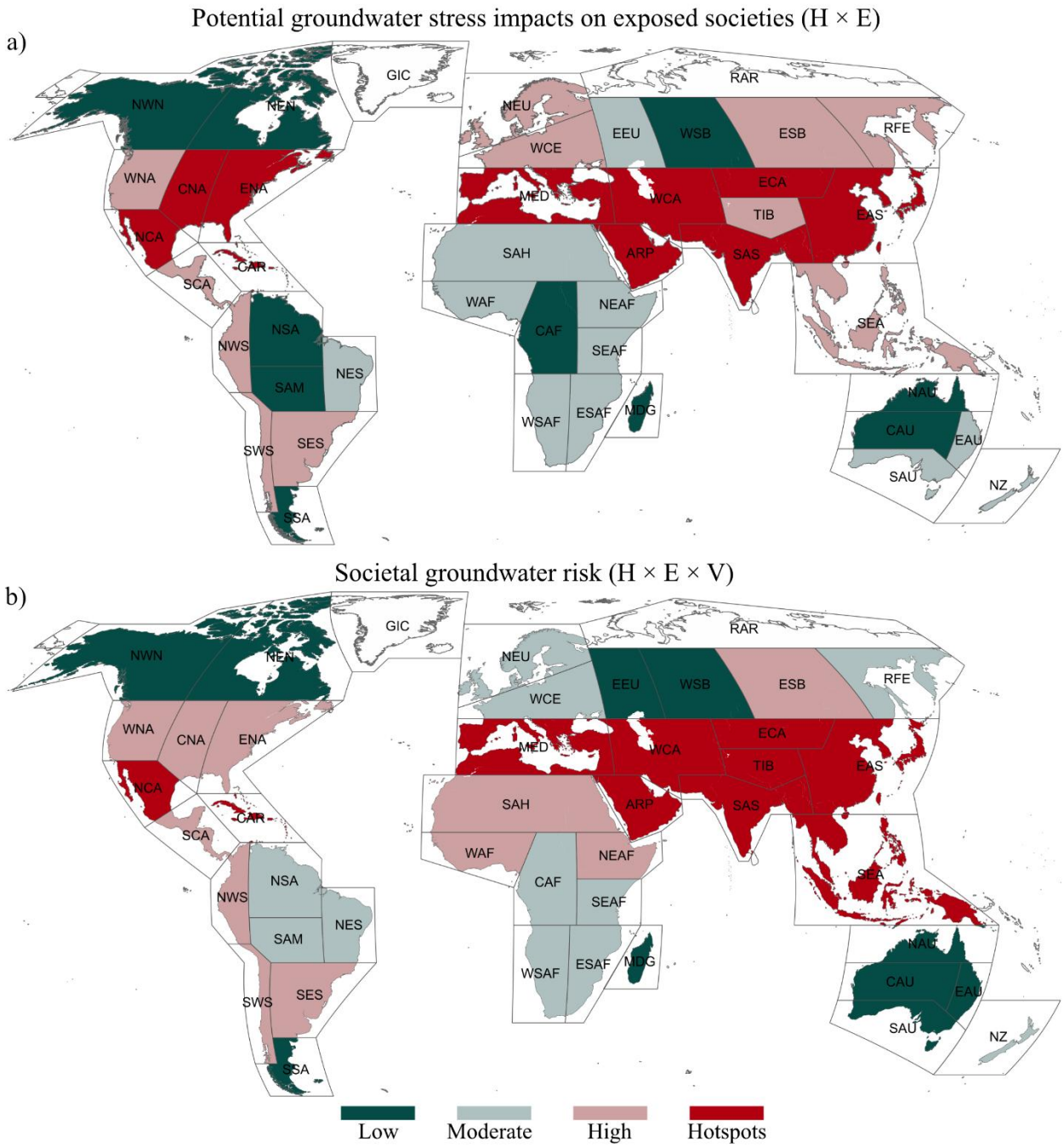

Supplementary Fig. 3. Role of vulnerability in shaping global groundwater risk.

(a) Potential groundwater stress impacts on exposed societies, represented by the product of groundwater stress hazard and societal exposure (H × E), aggregated to IPCC WGI reference regions (v4)[33]. (b) Societal groundwater risk, integrating groundwater stress hazard, exposure, and vulnerability (H × E × V), shown for the same regions. In both panels, values are classified into four categories based on quartiles of the global distribution, with the upper quartile indicating hotspot regions. The comparison highlights how incorporating vulnerability alters the spatial pattern and intensity of groundwater risk across regions.

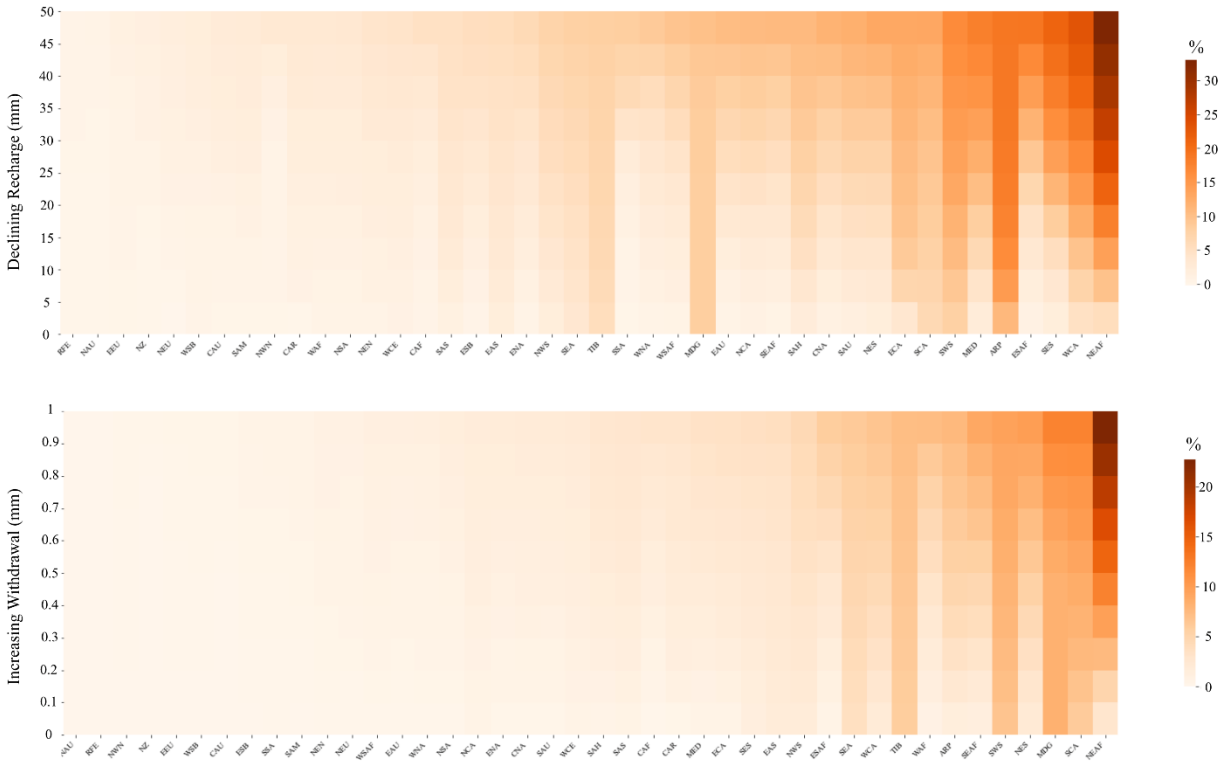

Supplementary Fig. 4. Sensitivity of groundwater risk to declining recharge and increasing withdrawals.

The upper panel shows the sensitivity of groundwater risk to reductions in recharge, and the lower panel shows sensitivity to increases in groundwater withdrawals. For each IPCC WGI reference region (version 4)[33]**,** the heatmaps indicate the increase in the number of grid cells entering the hotspot zone, defined as the upper 25% of the current global groundwater-risk distribution, under incremental decreases in recharge (mm) and increases in groundwater withdrawal (mm).

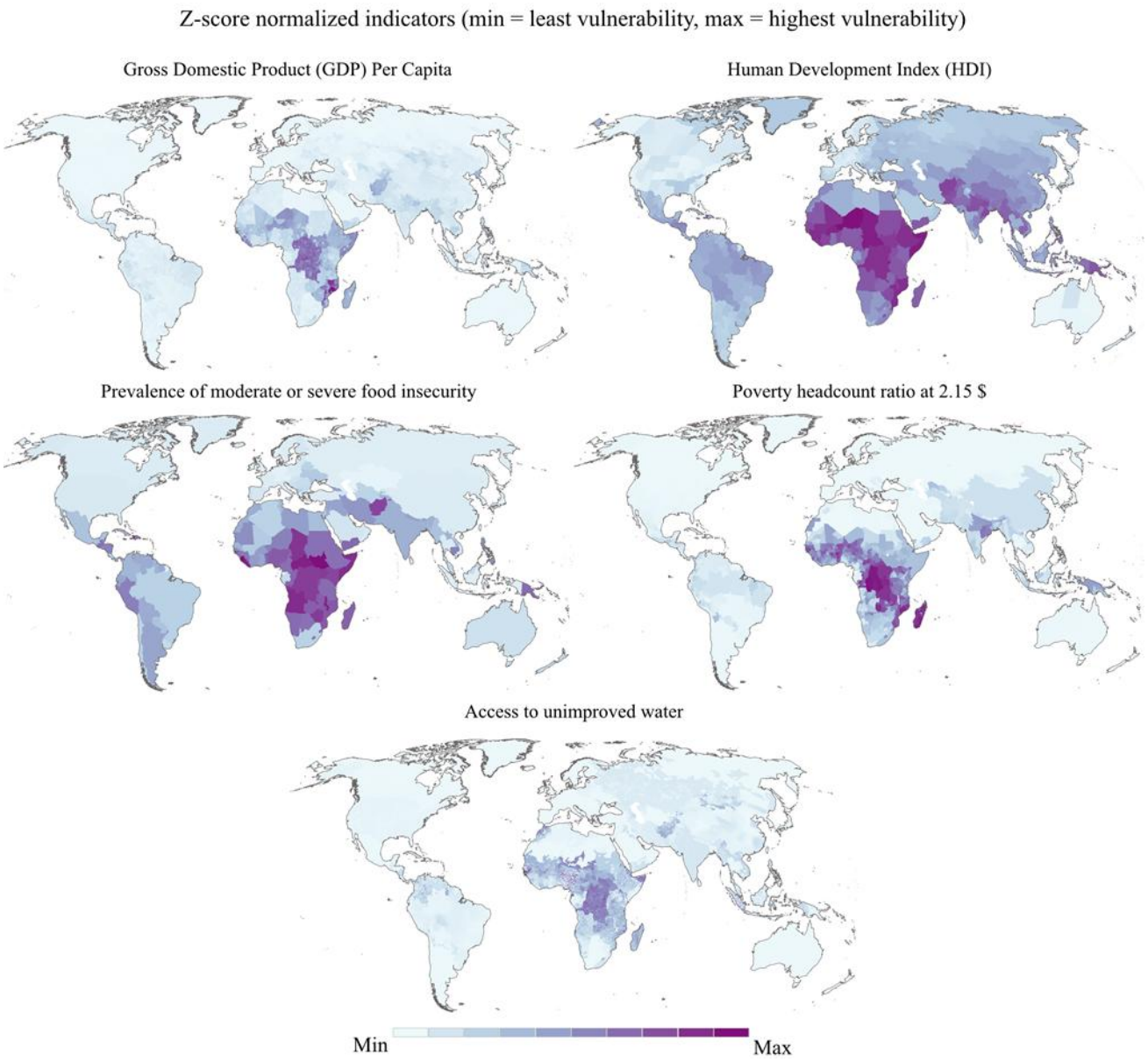

Supplementary Fig. 5.Indicators used for estimation of the socio-economic resilience dimension of vulnerability.

Spatial distribution of the indicators used to evaluate the socio-economic resilience dimension of the global groundwater risk framework including: Gross Domestic Product (GDP) per capita[19], Human Development Index (HDI)[20], prevalence of moderate or severe food insecurity[21], poverty headcount ratio at 2.15 USD[22], access to unimproved water[4,23].

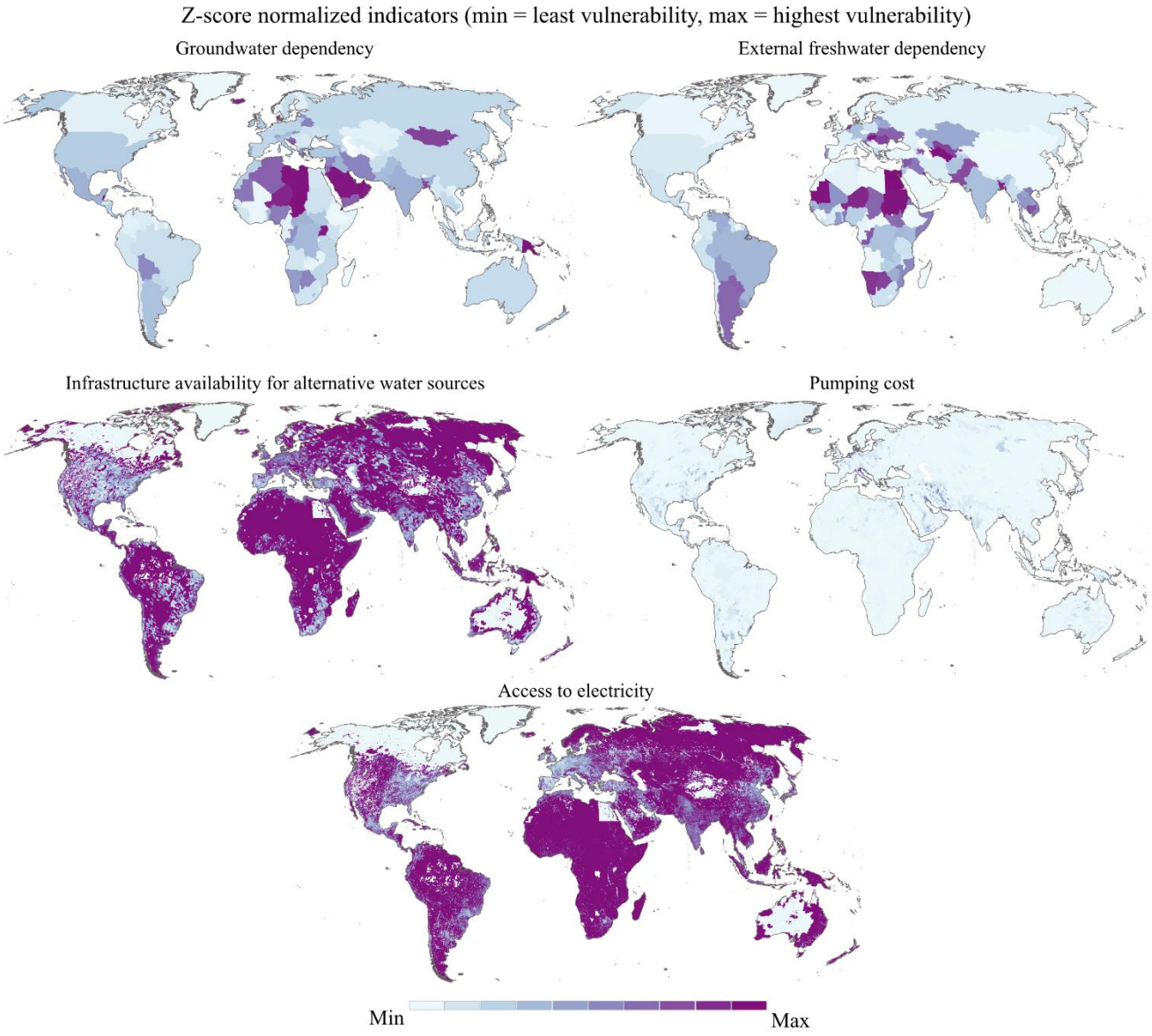

Supplementary Fig. 6. Indicators used for estimation of the water and resources dependency dimension of vulnerability.

Spatial distribution of the indicators used to evaluate the water and resources dependency dimension of the global groundwater risk framework including: groundwater dependency[34,35], external freshwater dependency[34], infrastructure availability for alternative water sources[24,25,27], pumping cost[36], access to electricity[28,37].

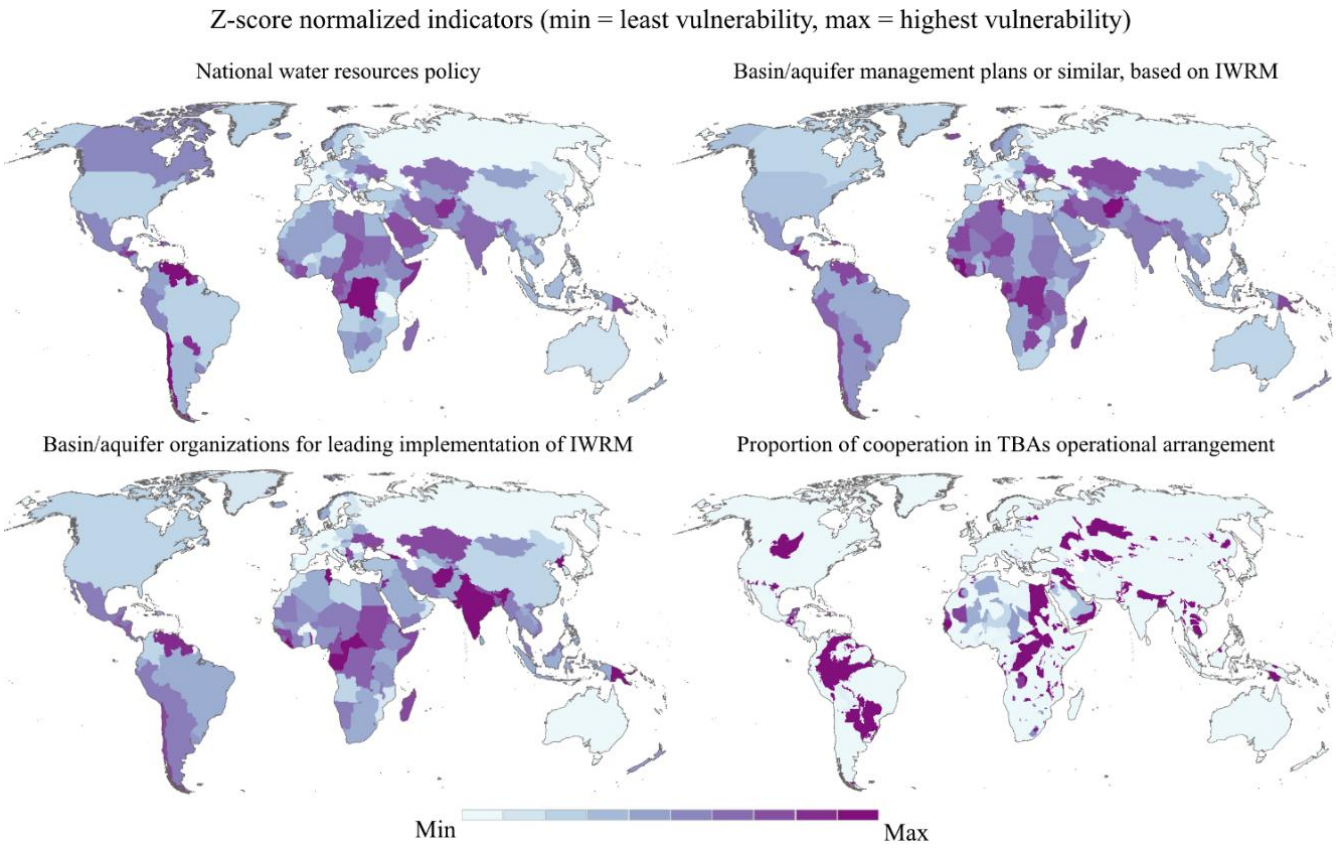

Supplementary Fig. 7. Indicators used for estimation of the water governance frameworks.

Spatial distribution of the indicators used to evaluate the water governance frameworks dimension of the global groundwater risk framework including: national water resources policy[38], basin/aquifer management plans[38], basin/aquifer organizations for IWRM implementation[38], and proportion of cooperation in transboundary aquifer operational arrangements[39,41].

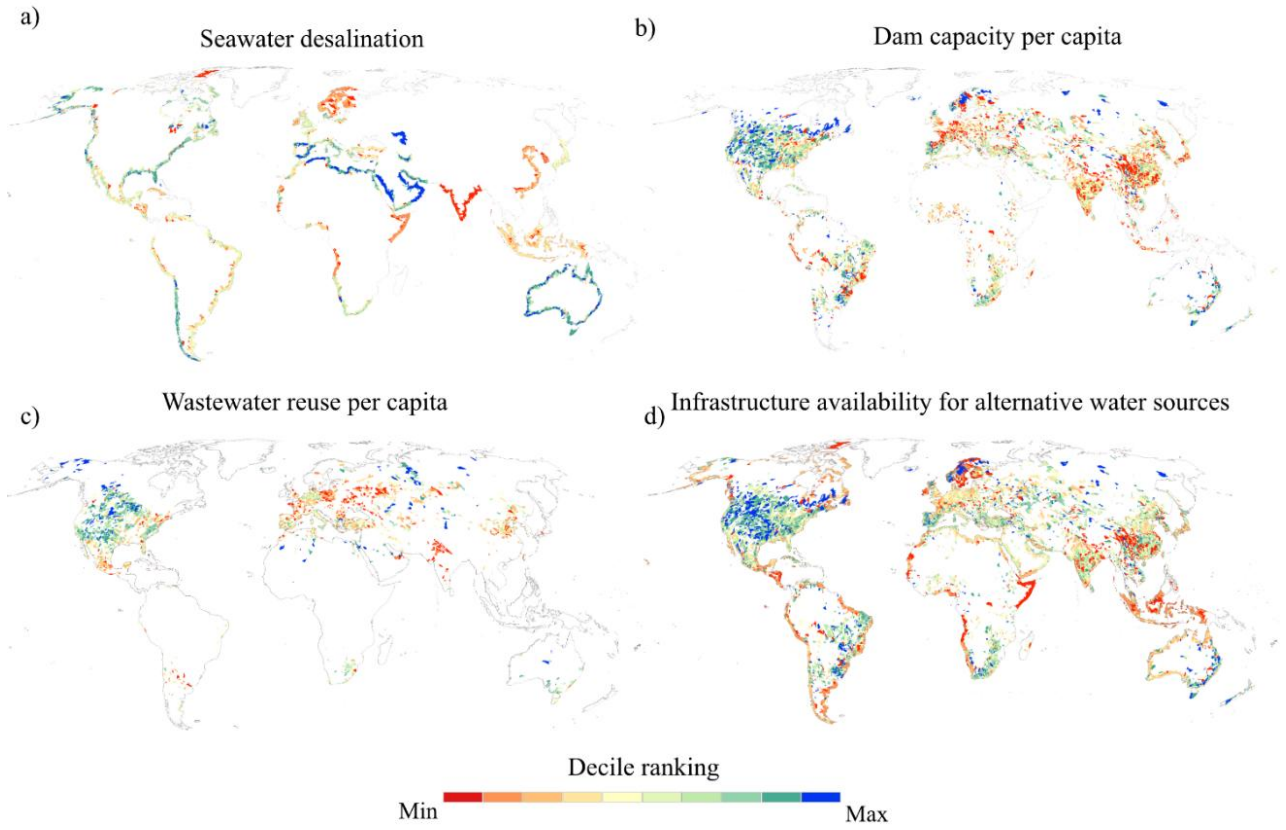

Supplementary Fig. 8. Infrastructure Availability for Alternative Water Sources.

Decile ranking of (a) desalinated water production [25,26], (b) dam capacity per capita [24], and (c) wastewater reuse [27]. d) Infrastructure availability for alternative water sources (This study).

References

1 UNISDR. Hyogo Framework for Action 2005–2015: Building the Resilience of Nations and Communities to Disasters. *United Nations International Strategy for Disaster Reduction, Geneva* (2005).

2 Carrão, H., Naumann, G. & Barbosa, P. Mapping global patterns of drought risk: An empirical framework based on sub-national estimates of hazard, exposure and vulnerability. *Global Environmental Change* **39**, 108-124 (2016).

3 Gill, J. C. *et al.* Concept note: The multi-hazard context and its relevance to the UN Office for Disaster Risk Reduction / International Science Council's Hazard Information Profiles (HIPs). *Zenodo* (2025). https://doi.org/10.5281/zenodo.15574444

4 Kuzma, S. *et al. Aqueduct 4.0: Updated decision-relevant global water risk indicators*. (World Resources Institute Washington, DC, USA, 2023).

5 Rossi, L. *et al. European drought risk atlas*. (European Commission, 2023).

6 Mittermaier, D. *et al.* The Climate Conflict Vulnerability Index (CCVI) - Technical Documentation v1.5. *Available online at climate-conflict.org* (2025).

7 Nardo, M. *et al. Handbook on constructing composite indicators: methodology and user guide*. (OECD publishing, 2008).

8 Ajtai, I. *et al.* Mapping social vulnerability to floods. A comprehensive framework using a vulnerability index approach and PCA analysis. *Ecological Indicators* **154**, 110838 (2023).

9 Greco, S., Ishizaka, A., Tasiou, M. & Torrisi, G. On the methodological framework of composite indices: A review of the issues of weighting, aggregation, and robustness. *Social indicators research* **141**, 61-94 (2019).

10 Abdrabo, K. I. *et al.* An integrated indicator-based approach for constructing an urban flood vulnerability index as an urban decision-making tool using the PCA and AHP techniques: A case study of Alexandria, Egypt. *Urban Climate* **48**, 101426 (2023).

11 Abson, D. J., Dougill, A. J. & Stringer, L. C. Using principal component analysis for information-rich socio-ecological vulnerability mapping in Southern Africa. *Applied Geography* **35**, 515-524 (2012).

12 Iqra, N. A. *et al.* Environmental vulnerability assessment in the south-west coastal region of Bangladesh using principal component analysis. *Coastal Engineering Proceedings*, 24-24 (2020).

13 Aung, T. S., Fischer, T. B. & Wang, Y. Conceptualization of health and social vulnerability of marginalized populations during Covid-19 using quantitative scoring approach. *Journal of Immigrant & Refugee Studies* **20**, 1-16 (2022).

14 Török, I. Qualitative assessment of social vulnerability to flood hazards in Romania. *Sustainability* **10**, 3780 (2018).

15 Kaiser, H. F. & Rice, J. Little jiffy, mark IV. *Educational and psychological measurement* **34**, 111-117 (1974).

16 Snedecor, G. W. & Cochran, W. G. Statistical Methods, eight edition. *Iowa state University press, Ames, Iowa* **1191**, 22 (1989).

17 Wu, T. Quantifying coastal flood vulnerability for climate adaptation policy using principal component analysis. *Ecological Indicators* **129**, 108006 (2021).

18 Bartlett, M. S. Tests of significance in factor analysis. *British journal of psychology* (1950).

19 Kummu, M., Kosonen, M. & Masoumzadeh Sayyar, S. Downscaled gridded global dataset for gross domestic product (GDP) per capita PPP over 1990–2022. *Scientific Data* **12**, 178 (2025).

20 Kummu, M., Taka, M. & Guillaume, J. H. Gridded global datasets for gross domestic product and Human Development Index over 1990–2015. *Scientific data* **5**, 1-15 (2018).

21 FAO. (2025).

22 World Bank. (2023).

23 Deshpande, A. *et al.* Mapping geographical inequalities in access to drinking water and sanitation facilities in low-income and middle-income countries, 2000–17. *The Lancet Global Health* **8**, e1162-e1185 (2020).

24 Lehner, B. *et al.* The Global Dam Watch database of river barrier and reservoir information for large-scale applications. *Scientific Data* **11**, 1069 (2024).

25 Hanasaki, N., Yoshikawa, S., Kakinuma, K. & Kanae, S. A seawater desalination scheme for global hydrological models. *Hydrology and Earth System Sciences* **20**, 4143-4157 (2016).

26 Ai, Z., Ishihama, F. & Hanasaki, N. Mapping current and future seawater desalination plants globally using species distribution models. *Water Resources Research* **58**, e2021WR031156 (2022).

27 Jones, E. R., Van Vliet, M. T., Qadir, M. & Bierkens, M. F. Country-level and gridded estimates of wastewater production, collection, treatment and reuse. *Earth System Science Data* **13**, 237-254 (2021).
28 CIESIN. (Center for International Earth Science Information Network - CIESIN - Columbia University, NASA Socioeconomic Data and Applications Center (SEDAC), Palisades, New York, 2018).
29 Kumar, R. *et al.* Multi-model assessment of groundwater recharge across Europe under warming climate. *Earth's Future* **13**, e2024EF005020 (2025).
30 Reinecke, R. *et al.* Uncertainty of simulated groundwater recharge at different global warming levels: a global-scale multi-model ensemble study. *Hydrology and Earth System Sciences* **25**, 787-810 (2021). https://doi.org/10.5194/hess-25-787-2021
31 Nazari, S., Reinecke, R. & Moosdorf, N. Global sectoral groundwater withdrawal: estimates and uncertainty analysis [dataset]. *PANGAEA* (2025). https://doi.org/pangaea.de/10.1594/PANGAEA.982842
32 Nazari, S., Reinecke, R. & Moosdorf, N. Global estimates of groundwater withdrawal trends and uncertainties. *Environmental Research Letters* (2025).
33 Iturbide, M. *et al.* An update of IPCC climate reference regions for subcontinental analysis of climate model data: definition and aggregated datasets. *Earth System Science Data Discussions* **2020**, 1-16 (2020). https://doi.org/10.5194/essd-12-2959-2020
34 FAO. AQUASTAT Core Database. Food and Agriculture Organization of the United Nations. Database accessed on [2023/06/29]. (2023).
35 Nazari, S., Reinecke, R. & Moosdorf, N. Global estimates of groundwater withdrawal trends and uncertainties. *Environmental Research Letters* **20** (2025). https://doi.org/10.1088/1748-9326/adf6ca
36 Niazi, H. *et al.* Long-term hydro-economic analysis tool for evaluating global groundwater cost and supply: Superwell v1. 1. *Geoscientific Model Development* **18**, 1737-1767 (2025).
37 Hu, T. *et al.* Modeling the spatiotemporal dynamics of global electric power consumption (1992–2019) by utilizing consistent nighttime light data from DMSP-OLS and NPP-VIIRS. *Applied Energy* **322**, 119473 (2022).
38 UNEP and UNEP-DHI. (2024).
39 United Nations. (Department of Economic and Social Affairs, 2024).
40 IGRAC. (International Groundwater Resources Assessment Centre (IGRAC), Delft, Netherlands, 2020).
41 IGRAC. (International Groundwater Resources Assessment Centre (IGRAC), Delft, the Netherlands, 2024).